بسم الله الرحمن الرحيم

Sudan University of Science & Technology

College of Graduate Studies

Human Generated Power by Using Piezoelectric Transducer

(Simulation Study)

إستخدام طاقة الإنسان في توليدالطاقة الكهربائية بواسطة مبدل

بيزوكهربي (دراسة محاكاة)

A Thesis Submitted in the partial fulfillment for the Requirements of the degree of M.Sc. in Mechatronics Engineering

By:

Tasabeeh Khalid Mohamed Farag

(B.Sc. (HONORS) in Electrical Engineering)

Supervisor: Dr. El Khawad Ali El Faki

September2016

الايـــة

قـال تـعـالـي:

(وَسَخَّرَ لَـكُمْ مَـافِـي
الـسَّمَـاوَاتِ وَمَـا فِـي
الأَرْضِ جَمِيـعًـا مِـنْهُ إِنَّ
فِـي ذَلِـكَ لآَيَـاتٍ لقِـَوْمٍ
يَـتَـفَـكَّـرُونَ)

صدق الـلـه الـعظيم

[الـجـاثـيـة: 13]

DEDICATION

This project is dedicated to...
My beloved **Mother** and **Father** and for my **grandmother soul**
For their endless love, support and encouragement.
My dear **Brother and Sister**
For helping me in the whale stages to finish my humble work.
And for my best colleague ever **Emad Eldein al taj** for helping me to manage my work while studying to finish my thesis.

Acknowledgement

I am thankful to Almighty **ALLAH**, most gracious, who In his infinite mercy has guided me to complete this Master Thesis.

Special appreciation goes to my supervisors **Dr. Mussab Hassan Zaroug** in guiding me in chapter one and two, and great appreciation goes to **Dr. El Khwad Ali El faki** for the supervision and constant support to finish the final form of my thesis, and for their both valuable constructive comments and suggestions throughout this research.

Abstract

The importance of using a human energies to charge electronic devices have increased in recent decades at a faster rate than it was with previous decades, studies have shown that human power is the ability(energy)to be produced by the human body. Power comes primarily from muscles, but body heat is also used to do work like warming shelters, food, or other humans. World records of power performance by humans are of interest to work planners and work-process engineers. The average level of human power that can be maintained over a certain duration of time, say over the extent of one minute or one hour is interesting to engineers designing work operations in industry. Human power is sometimes used to generate electricity that is stored. This research concentrated on the study of how to use the kinetic energy or heat for humans to charge small electronic devices, where the model has been designed using a variety of materials; Then the energy required for different applications was calculated for charging electronic devices using piezoelectric element was eventually put a number of proposals to increase the amount of energy produced from the work induced, especially of walking.

مستخلص

تزايدت في العقود الاخيرة اهمية استخدام احد طاقات الانسان لشحن الاجهزة الاكترونية بمعدل اسرع مما كان علية بالعقود السابقة والدراسات اثبتت بان القوة البشرية هي القدرة أو الطاقة التي يتم إنتاجها من جسم الإنسان.

وأظهرت الدراسات السابقة بأن قوة الإنسان هي القدرة أو الطاقة التي يتم إنتاجها من قبل الجسم البشري. تأتي القوة في المقام الأول من العضلات، وايضا استخدام حرارة الجسم أيضا للقيام بتدفئة الملاجئ والغذاء، أو غيره. الأرقام القياسية العالمية للطاقة من قبل البشر اصبحت من اهتمام المخططين والمهندسين. متوسط مستوى القوة البشرية التي لا يمكن الحفاظ عليه على مدى فترة معينة من الزمن، كمثال على مدى دقيقة واحدة أو ساعة واحدة مثيرة للاهتمام للمهندسين تصميم عمليات الأعمال في الصناعة. يستخدم القوة البشرية في بعض الأحيان لتوليد الكهرباء التي يتم تخزينها.

في هذا البحث تمت دراسة كيفية استخدام الطاقة الحركية او الحرارية للانسان لشحن الاجهزة الالكترونية الصغيرة حيث تم تصميم النموذج باستخدام مجموعة مختلفة من المواد ; ثم تم حساب الطاقة اللازمة لعدة تطبيقات مختلفة لشحن اجهزة الكترونية باستخدام مبدل اجهادي وفي النهاية تم وضع عدد من الاقتراحات لزيادة كمية الطاقة المنتجة من الشغل الحركي الذي يبذله الانسان خصوصا من المشي.

TABLE OF CONTENT

List of Tables

List of Figures

List of Symbols and abbreviation

F_{ext}	the external acceleration input due to the foot motion
$F_{Air}(x, \dot{x})$	the forces due to air compression
$F_R(\dot{x})$	friction forces
F_e	the electrical damping force
k	the coupling coefficient
φ	the magnetic flux
x	the axis of motion
U_{ind}	the voltage induced in the coils
B	the magnetic flux density
A	the cross-sectional area of the coil
$J\ddot{\varphi}$	equal to the sum of all torsional moments in the system
m_{tot}	the total mass in the system
L_{eff}	the effective length with respect to the center of gravity of the total mass
A	the excitation acceleration
$F_{d,e}$	the electrical damping force
$F_{d,m}$	the mechanical damping force
L_d	the distance
J	accounts for either electrical or mechanical damping forces
C_F	the coupling factor
I	the current in the coil
$R_{in} + R_L$	damping element
E	Energy
C	Capacitance
V	Voltage(Potential Energy)

Chapter One

Introduction

Chapter One
Introduction

1.1 General Introduction

The usefulness of most high technology devices such as cell phones, computers, and sensors is limited by the storage capacity of batteries. In the future, these limitations will become more pronounced as the demand for wireless power outpaces battery development which is already nearly optimized [3]. Thus, new power generation techniques are required for the next generation of wearable computers, wireless sensors, and autonomous systems to be feasible. Piezoelectric materials are excellent power generation devices because of their ability to couple mechanical and electrical properties. Consequently, when a piezoelectric is strained it produces an electric field; therefore, piezoelectric materials can convert ambient vibration into electrical power. Piezoelectric materials have long been used as sensors and actuators; however their use as electrical generators is less established. A piezoelectric power generator has great potential for some remote applications such as in vivo sensors, embedded MEMS devices, and distributed networking. Developing piezoelectric generators is challenging because of their poor source characteristics (high voltage, low current, high impedance) and relatively low power output.

In this project the first step was to generate electrical power as non-conventional method by simply walking or running on the foot step. Non-conventional energy system using foot step is very essential because it converts mechanical energy into the electrical energy. As much as possible, I tried to avoid using dynamos which produce more electricity but the idea is to use one of human generated power source to generate an electrical signal or voltage, don't forget mentioning that dynamos will create a lot of noise. Thus during looking for information and browsing the scientific research papers and online scientific paper I found that I can use a piezoelectricity. This is just a thesis science experiment that will show you the concept of producing electricity using piezoelectric element.

Electricity to power mobile technologies must be available at all times and the source of that must come on the individual scale to allow for freedom from being corded to an outlet. The solution lies in using piezoelectric materials to generate electricity through harvesting the energy expended through walking [1].

Based on information gathered through researching previous work in the field of regenerative electricity it can be determined that electricity conversion through the usage of piezoelectric materials seems to be the most practical for implementation on a large scale. The goals for the project include constructing a system which can harvest energy that is expended through walking in order to power low consumption mobile electronics. By replacing the conventional soles of a shoe with PZT material it is then possible to convert the mechanical energy in the form of heal strikes into electrical energy that can be stored through a linear low power collection unit. This power can then be used to provide electricity for devices that would otherwise rely on other primary and secondary batteries.

1.2 Problem Statement

The main intention is to use one of the forms of human generated power for mobile electronics to generate power to a mechatronics device with the aim of using piezoelectric transducer/sensor. The piezoelectric element is used to get the electric power that needed to charge a mobile electronic device circuit. The main problem in this part is to get the piezoelectric sensor and on how to attach it to achieve the desired power to charge the battery of electronics device.

1.3 Research Importance

To convert one of the forms of human generated power which is walking, using piezoelectric principle to generate power for mobile electronics and the design can eventually create clean, renewable electricity to charge portable devices like sensors, GPS units and cell phones.

1.4 Objectives

To study the output power of a power harvester using piezoelectric transducer model and to simulate the working principle of the power harvester by using Proteus 8 Professional and then display the power by visual LCD screen.

1.5 Methodology

The methodology used in this project is to determine the objectives of the project and how to achieve it. Secondly to collect more information about piezoelectricity so that to know more about the criteria of human generated power through the transducer and the application of it. Thirdly to review previous studies and researches in the area of harvesting any kind of human power using a piezoelectric transducer. Fourthly to choose

the piezoelectric transducer mechanism to achieve the best performance, then building actuator design and choose the best material and then building a simulated design to calculate the number of the steps that we need to power a cell phone battery.

1.6 Thesis Outlines

Chapter one includes introduction, problem statement, proposed Solution, objectives and methodology, Chapter two includes theoretical Background and literature review, Chapter three includes modeling of piezo electric transducer making power, block diagram, and system component, Chapter four contains the system simulation design result, and finally chapter five includes conclusion and recommendations.

Chapter Two

Literature Review

Chapter Two
Literature Review

2.1 Background

As mobile computing becomes a holdfast in the lives of the human population the need for a way to power these technologies also increases accordingly. With current sources of electricity limited to wall sockets reliant on a centralized location where electricity is generated a change in this system is a requirement for the advancement for technologies [1].

Modern compact and low power sensors and systems are leading towards increasingly integrated wearable systems. One key bottleneck of this technology is the power supply. The use of energy harvesting techniques offers a way of supplying sensor systems without the need for batteries and maintenance. In this work we present the development and characterization of two inductive energy harvesters which exploit different characteristics of the human gait. A multi-coil topology harvester is presented which uses the swing motion of the foot. The second device is a shock-type harvester which is excited into resonance upon heel strike. Both devices were modeled and designed with the key constraint of device height in mind, in order to facilitate the integration into the shoe sole. The devices were characterized under different motion speeds and with two test subjects on a treadmill. An average power output of up to 0.84 mW is achieved with the swing harvester [2].

In an increasingly mobile world it is the focus of research groups across different disciplines to achieve ever-improved miniaturization while also reducing the power consumption of devices and systems from sensors to wireless transceivers. These achievements gradually make a battery-free world appear more feasible as an increasing number of applications can be powered autonomously using energy harvesting devices, i.e. devices capable of generating energy out of what is available in their surrounding environment. The field of energy harvesting is comprised of various physical transduction types which can translate different forms of energy into electrical energy. The largest portion of devices presented so far focuses on harvesting kinetic energy, e.g. from machine vibrations. Energy harvesting for body-worn or body-attached applications has seen a significant amount of research interest as it can potentially provide the solution for powering modern low-power sensor systems and increase the mobility and independence of the user. Previous investigations have shown that several dozens of Watts are expended in the human gait which is a feasible energy source for human motion harvesters and will be the focus of this work. However, a wide range of challenges has to be dealt with in order to not only guarantee the technical functionality of the

harvesting device but also the applicability and the practical feasibility. From the application point of view, the power supply unit, including the energy harvester, power management and energy storage, has to provide a specified amount of energy for the operation of the application. This operation can be continuous or triggered at certain time intervals to fulfill its task. The harvester has to be designed accordingly. In turn this requires a certain minimal device size as the power output of the harvester system is directly related to the size of the electromechanical transducer. In the case of inductive harvesters this could for example translate into large magnets and in piezoelectric devices into a large number of active layers [13].

The aforementioned requirement of a certain device size is in conflict with the aspects of integration. In order to be able to integrate an energy autonomous system into clothing, the main technical obstacles to overcome are the device size2, its weight and the cost of the device. Hence a trade-off has to be found between a device size and transducer configuration which can fulfill the power requirements, but also satisfy the restrictions posed by the integration process. Depending on the particular application it might be necessary to develop a harvester rather large in size and weight, while on the other hand the device is expected to be small and lightweight to facilitate the integration as well as to retain wearing comfort. Additionally it depends upon the particular application how the device size is distributed. The obvious location to place a harvester within a shoe is in the shoe sole, therefore the longest dimension lies along the length of the shoe. The space along the width of the shoe is more limited and the height of the device is highly restricted, therefore a device would have to be comparatively flat, while there is some freedom with the choice of the surface area [1].

In the following section the key characteristics of the human gait are briefly outlined before an overview of previously presented human motion harvesters is given in section three. The fourth section describes the development of an inductive swing-type harvester that exploits the swing motion of the foot during walking. A shock-excited inductive harvester that exploits the impact of the foot with the ground is presented in the fifth section. A critical comparison of both types of human motion harvesters is then given in the concluding section [3].

2.2 Review of Industrial Piezoelectric Energy Conversion

Among the several energy conversion materials, piezoelectric materials are widely used for smart structures, normally classified into two different types based on the energy conversion direction. The first one is the actuator type, in which the piezoelectric element undergoes a

dimension change when an electric field is applied. The electric energy is converted into mechanical energy based on the indirect piezoelectric effect. The second type is called the sensor type, in which an electric charge is produced when a mechanical stress is applied. The micro-generator is based on:

• The mechanical-to-electrical energy conversion (that called direct piezoelectric effect).Expectations of energy harvesting must be realistic.
• Energy Harvesting Devices are already commercially available.
• Reduction of power requirements, particularly for wireless technologies has increased the opportunities for energy harvesting.
• Piezoelectric based energy scavengers offer very good performance in comparison to the other techniques especially in Microsystems applications. But integration challenge!

2.3 Human Gait as an Energy Source

The human gait exhibits three suitable sources of energy for energy harvesting devices, which are schematically depicted in figure 1. There are two acceleration-based excitation sources, namely the acceleration pulse upon heel strike, i.e. the impact between shoe and ground, and the acceleration due to the leg swing during walking. The other excitation source is the force that acts upon the shoe due to the weight of the person. As far as the force acting upon the shoe sole is concerned, previous investigations have shown that the force can dynamically amount to up to 130% of the person's body weight and therefore easily reach values of 1000 N.

This part focuses on the two acceleration-based excitation sources as potential energy sources for harvesting energy from the human gait. Therefore, acceleration measurements were performed at constant running velocities of 4 km h^{-1}, 6 km h^{-1}, 8 km $h^{-1}$and 10 km h^{-1} on a treadmill. A three-axis accelerometer was firmly attached to the sole at the back of a shoe. For a shoe lying flat on the floor, the *x*-axis of the acceleration sensor was in line with the vertical axis of the shoe pointing down to the ground whereas the *z*-axis was in line with the horizontal axis of the shoe. The accelerations were recorded with duration of one minute for each motion speed [8].

Figure 2.1 shows 5s time-frames of the recorded data along the mentioned axes. The data shown was recorded at speeds of 4 km h^{-1} in panes (a) and (b) and 10 km h^{-1} in panes (c) and (d) ,thus giving an overview of the acceleration patterns for both walking and jogging[8].

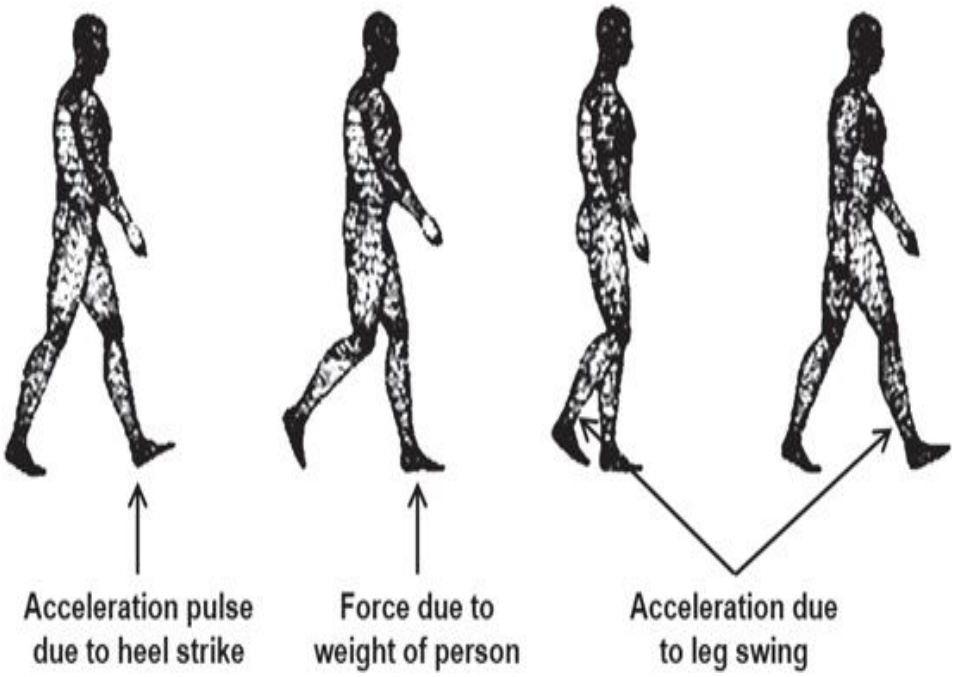

Figure 2.1: Schematic of the excitation conditions available in the human gait [7].

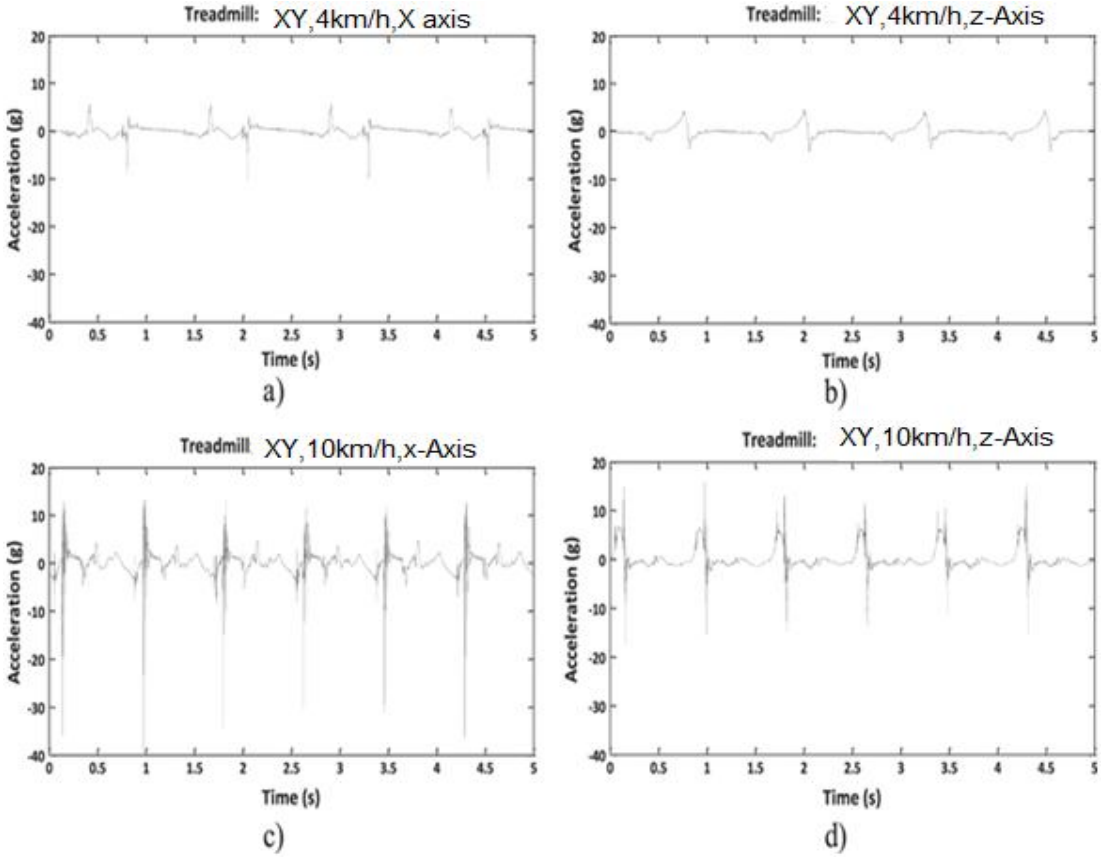

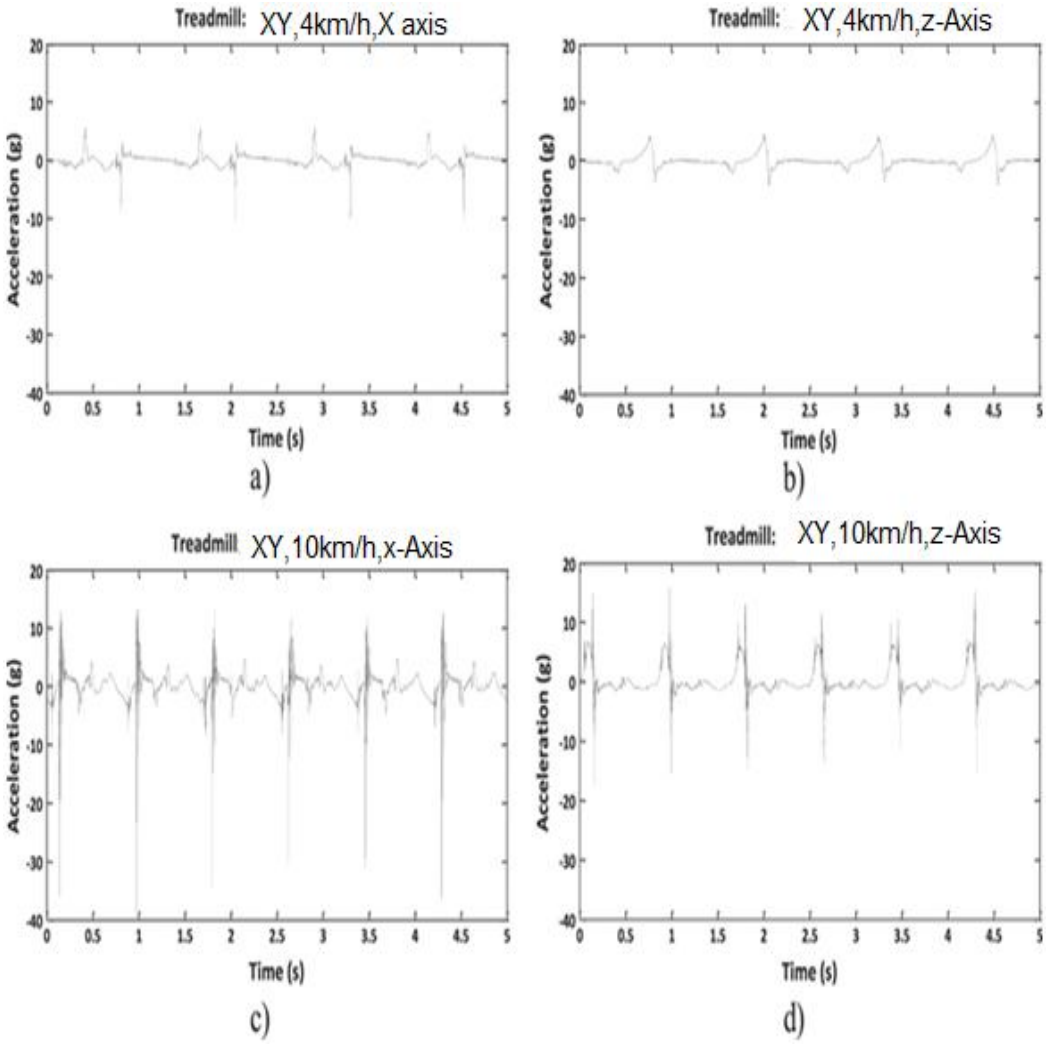

Figure 2.2 Recorded accelerations for runner 'XY'

The key observation made for the acceleration data is the large value of the acceleration peaks. On the vertical axis accelerations can peak at nearly 50 g while on the horizontal axis they can peak at approximately 20 g.

Table 2.1 summarizes the average acceleration peaks for the full data recordings for the *x* and *z* axis and two different runners respectively. On the *x* axis positive values correspond to a downward motion of the foot while on the *z*-axis the positive values correspond to a backward motion of the foot.

Table 2.1 Average acceleration peaks recorded during treadmill runs.

		Positive peak average (g)				Negative peak average (g)			
		Person XY		Person DH		Person XY		Person DH	
Motion speed		*x*-axis	*z*-axis	*x*-axis	*z*-axis	*x*-axis	*z*-axis	*x*-axis	*z*-axis
4 km h^{-1}	(slow walking)	5.2	4.4	6.4	2.9	-10.2	-3.7	-10.5	-4.9
6 km h^{-1}	(fast walking)	7.9	5.8	5.5	5.3	−21.7	−6.6	−16.3	−5.8
8 km h^{-1}	(slow jogging)	8.8	8.1	4.7	6.1	−27	−10	−21.6	−7.8
10 km h^{-1}	(fast jogging)	13	13	9	9.7	−33.5	−13.7	−33.6	−11.4

Two different runners with different body geometries were recorded with runner DH being lighter and taller, while runner XY is heavier and smaller. While these values are of limited statistical significance as they represent only two person's walking style and body geometry, the magnitudes of the accelerations indicate the applicability as an excitation source for energy harvesters.

A distinctive feature of walking is the very low frequency at which successive footsteps occur. As shown in table 2.2. Step frequencies for two persons at various motion speeds. The step frequency of one foot varies between 0.8 Hz and 1.2 Hz as a function of motion speed. It can be seen that there is only a moderate increase in the step frequency with increasing motion speed. Towards higher motion speed the increase in step frequency diminishes, implying that it is the step length which has to increase to allow faster motion.

Table2.2 Step frequencies for two persons at various motion speeds.

Motion speed		Step frequency: person XY	Step frequency: person DH
4 km h^{-1}	(slow walking)	0.82 Hz	0.8 Hz
6 km h^{-1}	(fast walking)	1 Hz	0.94 Hz
8 km h^{-1}	(slow jogging)	1.18 Hz	1.2 Hz
10 km h^{-1}	(fast jogging)	1.19 Hz	1.19 Hz

Due to the low excitation frequency, a potential harvesting device cannot be continuously operated in resonance mode (i.e. excitation frequency equal to Eigen-frequency of energy harvester) as it is typically possible with machine vibrations of higher frequencies. Therefore, other concepts must be chosen, for example frequency up-conversion techniques or non-resonant techniques so that will not have difference on the frequency of the joggers as shown in the table.

2.4 Reported Devices

2.4.1 Force-Driven Harvesters

The large forces available upon heel-strike have motivated the development of several force-driven energy harvesting devices. The bending of piezoelectric materials attached to the shoe sole, both ceramics and polymer-based, was employed early on [11] leading to average power outputs of 1.8 mW and 1.1 mW respectively for a walking frequency of 1 Hz.

A generator using a lever and mechanical gears to translate the downward motion of the foot into a rotational motion coupled into a classical generator was also presented in [13]. While the device was rather large and heavy, it was able to generate an average power of 230 mW. A different approach employs the turboelectric effect, which is based upon materials of different electrochemical potential coming into contact, to generate maximum power outputs of up to 4.2 mW with a stacked structure which was pressed by a human palm [9]. Further force-driven devices can be found in [10].

2.4.2 Acceleration-Driven Harvesters

Particularly concerning the acceleration impulses available upon heel-strike, there has been only limited work. In [13] a piezoelectric macro scale prototype is presented. A heavy cylindrical mass is set into motion when the foot is lifted to form an angle with the ground. Magnets attached to piezoelectric beams snap towards this mass when it comes into range and vibrate freely at their resonance frequency, when released. This large device was able to generate a maximum power output of 2.1 mW at an excitation of 2 Hz in a laboratory setup. A second device incorporates a shoe-mounted piezoelectric vibrating cantilever and was presented in [14]. In this device the mass attached to a piezoelectric cantilever is displaced when excited by the acceleration impulses induced

by heel strike. The corresponding spring-mass system then starts to vibrate at its eigen-frequency. As a result, a classical damped response occurs at every heel-strike. A power output of about 14 W was achieved when walking at normal speed. By means of a sensitivity analysis based on a numerical model optimal parameters were identified, which provide the largest power output.

Using the optimum parameters a power output of 395 W was predicted. In both cases described, the energy harvester mechanism is based on a frequency up-conversion technique.

In the case of linear swing-type harvesters a number of devices have been reported. The shoe-integrated prototype upon which parts of this work are based was presented in [17] it consists of a single generating magnet that can swing freely within a PVC channel placed within the sole along the horizontal axis. Two coils are placed in precise positions in order to overlay the coils' voltage signals and double the output while requiring only one rectifying circuit. This device was able to generate average powers up to approximately 10.5 mW on a treadmill run at a velocity of 10 km h−1.

A different device based on the magnet-in-channel setup was presented in [16]. Different configurations of the coils, channels and magnets were investigated, leading to an average power output of up to 14 mW at a walking velocity of two steps per second (1 Hz) for the best configuration found. However, this device did not use synchronized coil signals and would therefore require multiple rectifying circuits for more than one coil when used in a sensor system.

The acceleration-driven harvesters mentioned so far have the common problem of a large device size which greatly reduces their acceptability for an integration in shoes which in turn is hardly possible without altering the shoes appearance. As a consequence it is of utmost importance to reduce the device size and particularly the height of the harvesters while trying to reduce scaling effects and the loss of generated power due to down-scaling in size.

2.5 Swing-Motion Harvester

This section describes a harvesting device which exploits the swing motion of the foot. A first rather large prototype was presented in [15]. On the basis of the previously gained experience the aim of this work is to develop a smaller device with particular focus on a reduced device height in order to facilitate the integration into shoes.

2.5.1 Design

For the miniaturized device a multi-coil configuration was chosen since a larger power output in contrast to a single coil design was expected. The magnets are concentrically placed in line separated by ferromagnetic steel spacers, creating an elongated stack as indicated in figure (2.3(a)). Two neighboring magnets always show opposing polarization. The repulsive flux lines are therefore forced into the spacer and guided sideways as shown schematically in figure (2.3(b)). This guarantees that each coil experiences several changes in direction of the magnetic flux within each step as several magnet-spacer sections pass by the coil. The coils are placed at equal intervals according to the distance between the magnets and connected in series. Because of this placement the magnets move through the coils simultaneously, i.e. every magnet enters a coil at the same time and with the same velocity. The alternating magnetic flux thus induces a voltage in every coil simultaneously, enabling the superposition of the voltage across the series connected coils, thereby reducing the requirements posed for the power management electronics, which in the simplest case can be a single rectifying circuit. Stopping magnets (SM) are introduced in order to prohibit the magnet stack from hitting the channel end at high velocities as this impact can clearly be felt in the shoe without cushioning and increases discomfort. As showing in stopping magnets at either channel end or Areas of high flux density marked in magenta. Coil positions indicated in red.

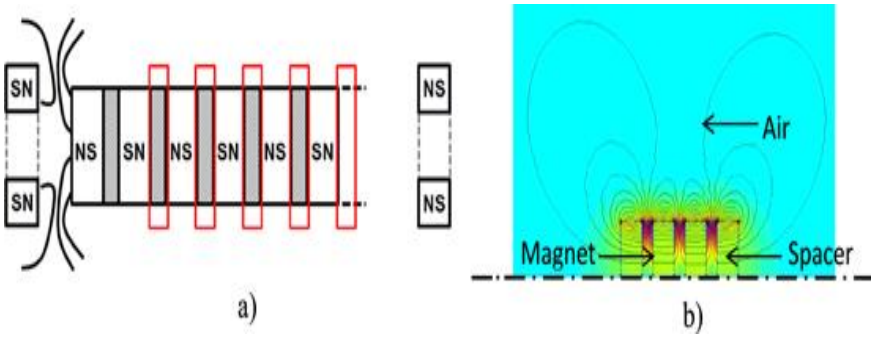

Figure 2.3 (a) Schematic of the magnet stacks. Magnets separated by spacers (gray). (b) FEM simulation showing the magnetic flux as it is guided through the spacers. [15].

2.5.2 System Model

The system model (figure 2.4) Follows the differential equation shown in (2.1). Apart from the real-world acceleration data, which is used as input to the system, a number of different forces acting upon the moving magnet are also considered.

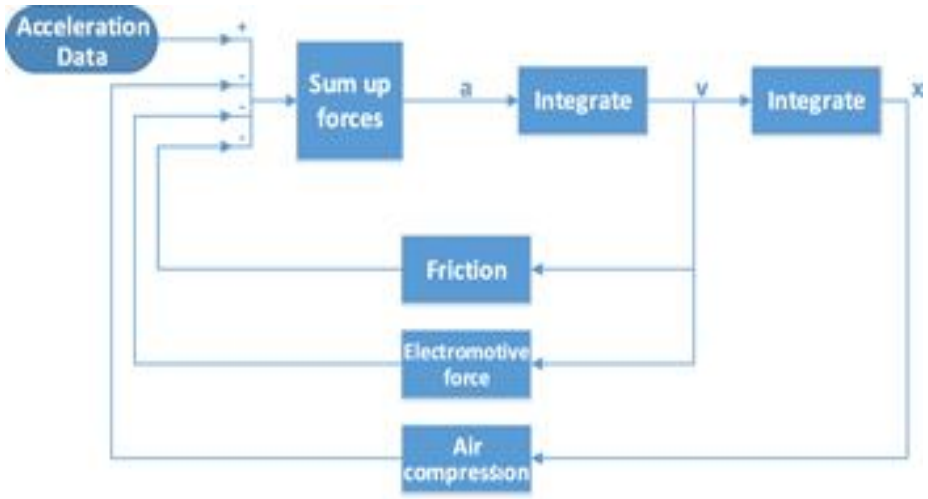

Figure 2.4 Block diagram showing the forces acting in the differential equation of the system model [15].

The friction forces between the magnet stack and the channel are calculated based on the weight of the magnet and the centripetal force built up during the swing motion of the foot, which acts as an additional normal force.

Air compression due to the air pushed in front of the magnet stack can be a highly limiting factor if no outlet is provided. In order to capture most of the magnetic flux within the coils, they are placed as closely to the magnets as possible. The channel is designed accordingly, leaving little space for air to pass by the magnet stack when it is moving. The model calculates the forces due to air compression by determining the volume change in the air pockets to the left and right of the magnet train at discrete time steps as the magnet moves. Thereupon one can estimate the exhaust velocity at the air outlet and the corresponding volume of air that is leaving the air pockets through the outlets. The differences in volume change between the air pockets and the corresponding differences in pressure can then be used to estimate the acting forces. Rubber stoppers were used in the fabricated setup and were modeled as a semi-elastic impact after first experiments showed that the influence of the SM on the moving magnet stack led to a greatly reduced range of motion.

As the magnet stack moves through the channel due to the external excitations, a voltage is induced in the surrounding coils and current flows through the coil windings. This current causes a magnetic field, which opposes the field of the magnet stack and thereby exerts a force on the magnets.

The equation of motion is given in (2.1) And considers the external acceleration input due to the foot motion F_{ext}, the forces due to air

compression $F_{Air}(x, \dot{x})$, friction forces $F_R(\dot{x})$and the electrical damping force F_e

$$m\ddot{x} = F_{ext} - F_{Air}(x, \dot{x}) - F_R(\dot{x}) - F_e\dot{x} \,. \qquad (2.1)$$

In order to determine the power generated in the coils and the electrical damping force, the spatial distribution of the magnetic flux density is calculated using FEM software. A steady-state axisymmetric problem is set up using the software FEMM. Asymptotic boundaries are defined at a distance of 2 cm from the magnet stack. The magnetic flux density is extracted from FEMM along the area corresponding to the coil area. The coupling coefficient is calculated using the FEM data according to equation (2.2), where *k* is the coupling coefficient,$\varphi$is the magnetic flux and *x* is the axis of motion:

$$K = -\frac{d\varphi}{dx} \,. \qquad (2.2)$$

The coupling coefficient reaches its highest values between two magnets where a change in the flux direction occurs (as shown below). A more detailed description of the calculation of the coupling coefficient and consequently the generated voltage can be found in (Electromagnetic Vibration Energy Harvesting Devices: Architectures, Design, Modeling and Optimization (Dordrecht, New York: Springer).

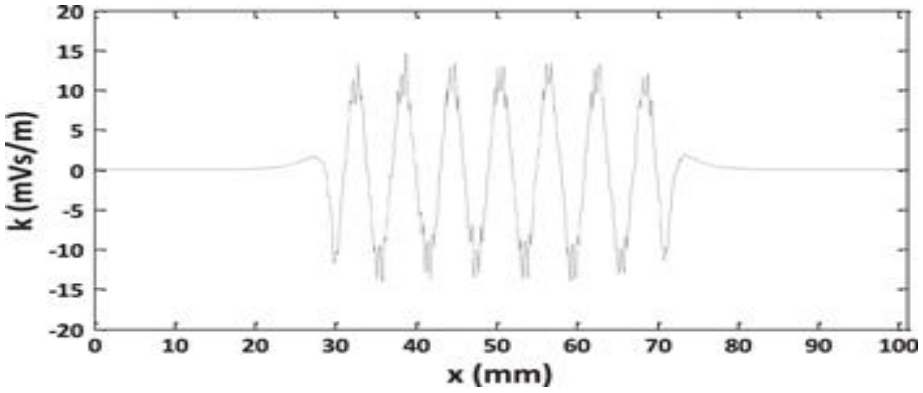

Figure2.5 Coupling coefficient *k* for the outer coil cells along the direction of the magnet stack. Simulation performed with a total of 14 magnets and 13 spacers.

The software model implemented in Matlab/Simulink calculates the motion of the magnet stack from the sum of the forces listed in equation

(2.1). the curve representing the spatial distribution of the coupling coefficient is shifted in position along the *x* axis, thus modeling the motion of the magnetic field. As the coils are placed in predetermined places and with fixed spacing, each coil experiences a separate magnetic flux depending on its location and generates a voltage according to equation (2.3), where U_{ind} is the voltage induced in the coils, B is the magnetic flux density and A is the cross-sectional area of the coil:

$$U_{ind} = -\frac{d\varphi}{dt} = -\left(\frac{dA}{dt}B + \frac{dB}{dt}A\right)_{|A=const}$$

$$= -\frac{dB}{dt}A.\frac{dx}{dx} = -\frac{dB}{dx}A.\frac{dx}{dt} = k.\dot{x}\ . \qquad (2.3)$$

The electrical damping force can be calculated using the coupling coefficient *k* and the current *i* induced in the coils according to equation (2.4):

$$F_e = i \cdot k\ . \qquad (2.4)$$

Each coil is divided into ten coil cells in order to represent the spatial extent of the coil more accurately. For each cell the value of the coupling coefficient at its location is determined, which improves the accuracy of the calculations. An optimum resistive load equal to the coil resistance (approximately 166 Ω) is used in the simulations.

2.5.3 Optimization

In order to meet the requirement of a reduced device height while generating the maximum power output, the magnet-in-channel model was optimized using the optimization software mode Frontier. The built-in multi-objective genetic algorithm 'MOGA-2' was used, which improves upon a given number of starting designs spread within the boundary conditions for a given number of generations to find the optimum design. The optimization was performed with a height constraint of 12.5 mm (15 mm including housing) and a length constraint of 62 mm (70 mm including housing).

The number of magnets to be used was determined by the optimization software. A trade-off has to be found between the number of magnets and the space available for magnet motion. A larger number of magnets greatly reduce the freedom of motion for the magnet stack. The completed optimization run resulted in a total of 14 magnets with a magnet height of 2 mm. Combined with the spacers the magnet stack forms a long cylinder of 41 mm in length. Two neighboring magnets always show opposing polarization. Table2.3 show the geometrical parameters of the multi-coil harvester. Although cylindrical magnets were

used in the system model, for practical reasons explained in the next section, ring magnets were chosen for the prototype device.

Table 2.3 Geometrical parameters of a multi-coil swing-type harvester [11].

Parameter	Value
Number of magnets	14
Magnet height	2 mm
Magnet outer diameter	7 mm
Magnet inner diameter	2.7 mm
Number of spacers	13
Spacer height	1 mm
Spacer outer diameter	7 mm
Spacer inner diameter	2.7 mm
Number of coils	13
Coil length	1.2 mm
Coil outer diameter	12.5 mm
Coil inner diameter	8.5 mm
Channel length	62 mm
Magnet stack length	41 mm

2.5.4 Implementation

Several difficulties were encountered during construction of the device. Gluing magnets together against the repulsive forces due to their opposing polarization proved very challenging. Several designs were investigated as shown in figure 2.6. The designs were simulated and the expected power output normalized to 100% for the best design is shown where large rectangles indicate magnets, small rectangles indicate spacers. The two graphs on the right show ring magnet configurations

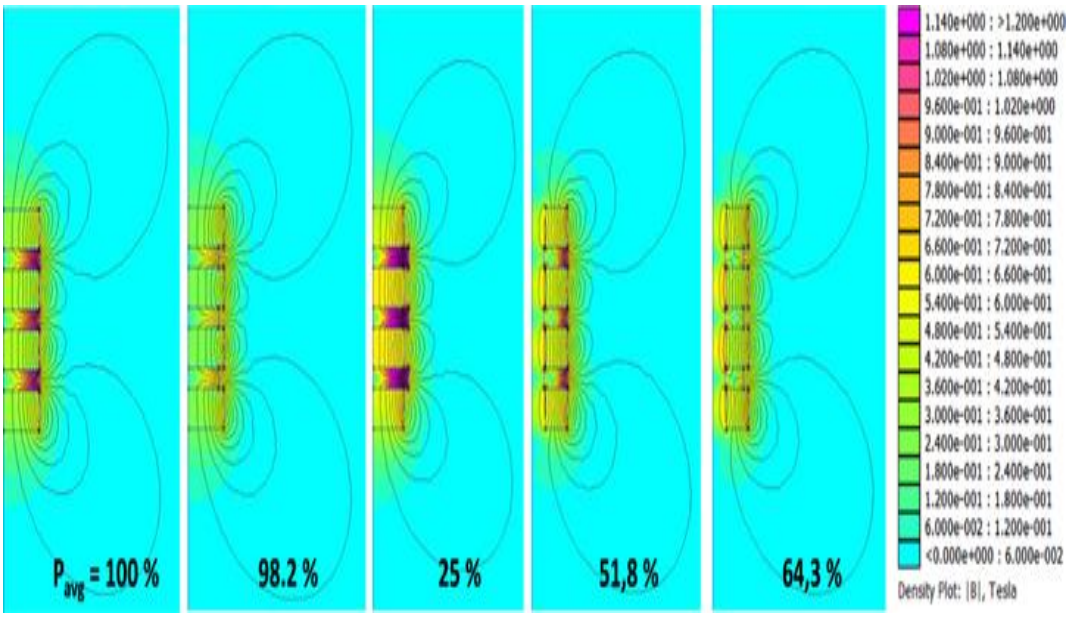

Figure 2.6 Different magnet stack configurations: rotational axis on the left border of the graphs [10].

The most practical design which uses ring-magnets and a supporting rod of non-ferromagnetic material in the free space at the center of the magnets shows a significant reduction in power output. Not only does this setup imply a reduced volume of active magnetic material but it also allows the magnetic field to partially short-circuit in the free space within the ring. This trade-off is acceptable for practical reasons, as it inherently allows the correct alignment of magnets and spacers with complete overlap. Additionally it facilitates the gluing process and especially when using a thread rod, the magnets can be held in place by screwing a nut onto either end of the rod. The fabricated prototype and its external placement on a shoe for characterization purposes are shown in figure 2.7.

2.5.5 Characterization

In order to analyze the performance of the device under real conditions, several treadmill runs were performed. A linear accelerator table was used for brief testing of the swing-type harvesters; however its attainable accelerations are limited to approximately $1 m s^{-2}$.Therefore the measured accelerations that occur during walking could not be replicated by other means than a treadmill.

As before, measurements were performed at four different motion speeds and for two runners of different body geometries. Figure 8 shows the measured power output of the harvester for runs performed on a treadmill and as a comparison for runs performed on the ground without a

treadmill. It was reported earlier that with the transition from the abrupt motions of fast walking to the rather smooth motions of slow jogging, a decrease in power output can be observed [15]. This effect can be observed in figure 8 as well, where the curves do not show a steadily ascending slope. The fact that for runner 'XY' this drop in power output occurs at lower motion speeds than is the case with runner 'DH' is attributed to the walking style and the body geometry of the runners. Measurements were also performed at a reduced set of motion speeds for walking without a treadmill. While treadmill runs offer a certain level of reproducibility, some differences can be expected when compared to walking on the ground.

First, on a treadmill one automatically makes alterations to the gait patterns in order to run smoothly. Second, the inherent spring-loaded characteristic of the treadmill causes the impact of the foot to be damped to a certain degree. An accelerometer is attached to the bottom of the harvester to synchronously record the accelerations.

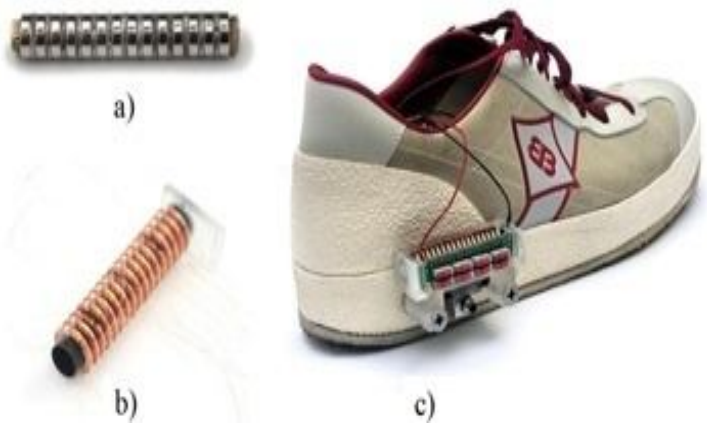

Figure 2.7 (a) Magnet stack mounted with nuts. (b) Multiple coils placed on plastic channel. (c) Harvester attached externally to the shoe in order to perform treadmill runs.

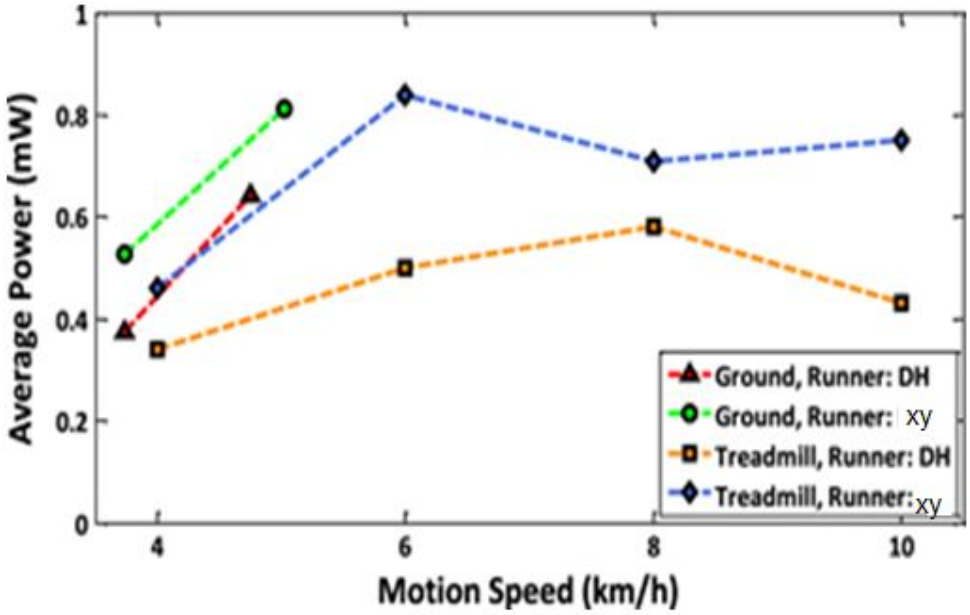

Figure 2.8 Power measurements for two runners at optimal load resistance (166).

Walking speed on the ground without treadmill is an approximate value. At the slowest measured speed of 4 km h−1on a treadmill, the harvester was able to generate 0.34 mW and 0.46 mW for the two runners. At approximately the same speed on the ground, power outputs of 0.375 mW and 0.526 mW were achieved. It can also be noticed that the maximum achieved power output of 0.81 mW for 'ground walking' is measured at 5 km h−1and thereby at a speed 1 km h−1slower than on a treadmill, where a nearly identical power output of 0.84 mW is achieved at 6 km h−1. It can therefore be assumed that the power output during normal walking without a treadmill is slightly larger than for treadmill runs, independent of the motion speed.

Figures2.9 (a) and (b) depict the measured voltage and power output respectively for approximately one step for runner XY at a speed of 6 km h-1. It can be seen from the figures that each step shows two characteristic impulses corresponding to the two major motions of the foot (forward and backward movement). Each waveform is made up from a number of consecutive peaks, which represent the change in flux direction between the coils of the magnet stack. The total energy per step can be obtained by integrating the power over one such step and its two impulses.

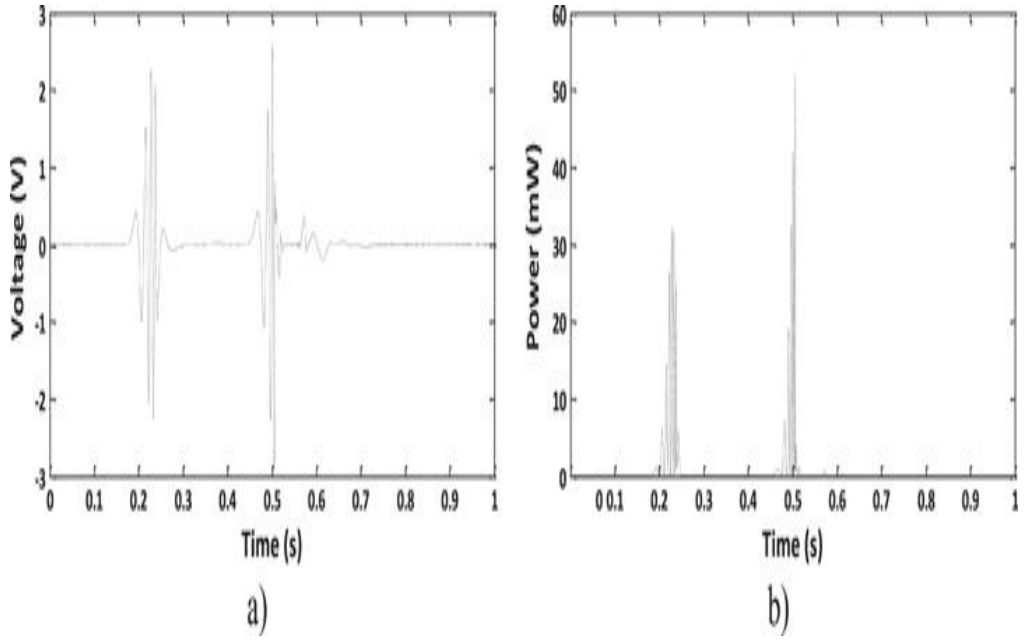

Figure2. 9(a) Enlarged section of the voltage output at a speed of 6 km h−1for runner XY. Each step shows two characteristic impulses, representing the two major foot motions. (b) Corresponding power output calculated from the voltage signal.

2.5.6 Discussion

The previous sections show that the miniaturization of a swing-type harvester through means of parallelization can be achieved without the devices power output dropping into unfeasible ranges. However, it has to be kept in mind that with a maximum recorded average power output of 0.84 mW the reduction due to scaling effects is significant as compared to [10]. The volume scales quadratically with the radius and thus the mass of the magnet stack, which is the inertial mass of this system, was greatly reduced from approximately 50 g in [10] to 9.8 g in this work. Not only does this result in reduced inertia of the magnet stack, but it also results in a reduced magnitude of the magnetic field due to the smaller magnets and consequently in a reduced power output. In practical terms the reduction in size is a great advantage, as the device with a total height of 15 mm including the housing is now far easier to incorporate into shoes. With a total length of 70 mm including housing it can also be integrated into the heel section of a shoe and is not negatively affected by the bending of the front part of the sole during walking.

Concerning the modeling of the device, a complete match between simulation and measurement for all velocities has not been achieved so far. Figure 10 shows a comparison between the simulated and measured power outputs for both runners. Apart from differences caused due to the

simple physics, errors are introduced by the discrete nature of the calculations performed, e.g. the magnetic flux density is calculated at fixed spatial intervals and used to determine a mean flux within each coil. The accuracy of this approximation depends on the step size. An increased resolution leads to a manifold increase in computing time as both the FEM simulation and Matlab have to perform an increased number of computations($t_{cak\sim resolution^2}$). Concerning the optimization algorithm which calculates hundreds of designs, a balance has to be found between computing time and accuracy. Additionally, it is assumed that the speed-dependent effects of the system model require further improvement.

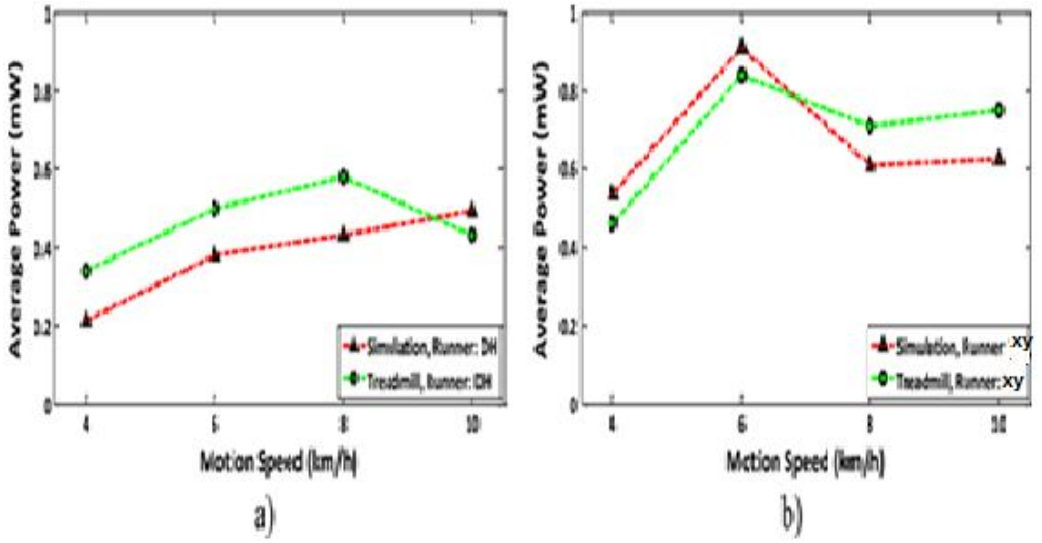

Figure 2.10 Comparison between simulated and measured power output shown for runner DH in pane (a) and runner XY in pane (b).

Therefore future work clearly includes improvements to the reproduction of real-world physics within the system model and the approximations used in the model, which continually leads to a better match between simulation and measurements. The influence of the calculation resolution on the model accuracy is not considered in this work.
The model was limited in flexibility as it was designed to simulate a fixed number of coils equal to the number of flux transitions between magnets. If the algorithm calculated a design with 14 magnets, the number of coils in the simulation would be set to 13. To avoid this limitation a fully flexible model is being worked on, which can calculate designs where the number of coils is independent from the number of magnets. Further improvement through a new design in a new optimization run is expected.

2.6 Shock-Excited Harvester

The second acceleration-based excitation source relates to the acceleration pulses upon heel-strike. A shock-excited energy harvester based on a frequency up-conversion technique appears to be a practical solution for converting acceleration pulses into usable electrical energy. In the following sections the design and characterization of such a device with dimensions of 60×40×20 mm3 is described.

2.6.1 Design and Parameter Optimization

As discussed for the swing-motion harvester, the usability of a device for energy harvesting from human motion depends strongly on its integration capability and thus on its size. Therefore, a strict constraint on the device size was also applied to the shock-excited energy harvester. For integration of the energy harvester into the heel of a shoe, the total height of the device must not exceed a limit of 20 mm. The width and length of the device were restricted to 40 mm and 60 mm, respectively. Applying these size constraints, an integration of the device into the heel of a shoe is feasible.

For converting the acceleration pulses into electrical energy an electromagnetic conversion mechanism was chosen. Due to the limited device height, the shock-excited energy harvester incorporates a magnetic circuit, which contains two air gaps. In this manner a reasonably flat design is achievable without losing too much volume for the active components (coil volume, magnet volume). A schematic diagram of the energy harvester structure (cross-section) including relevant design parameters is shown in figure (2.11(a)). The total width of the structure W_{total}, which is equal to 33 mm, follows from the total device width (40 mm) less the thickness of the housing and some air gap on both sides. The gap between coil and magnet was chosen to be 0.5 mm. The width of the coil W_{coil} follows from the dimensions of W_{sheet}, W_{mag} and the gap between magnet and coil. The height of the back iron sheet H_{sheet}, which is equal to two times the height of the magnet H_{mag}, is limited by the maximum height of the device and the internal displacement amplitude z_{max}. There will be a trade-off between the parameters H_{mag} and z_{max}. A large magnet height will increase the magnetic volume and the seismic mass. However, this is at the expense of the internal displacement amplitude.

A small internal displacement will induce impacts at the mechanical stoppers more often. The magnet height also depends on the availability of magnets with a particular height. In this first design, a magnet height of 5 mm was chosen resulting in a height of 10 mm for the back iron sheet. Considering a total device height of 20 mm and a thickness of the

housing of 2 mm, the internal displacement amplitude yields to 3 mm. The following design parameters are still variable and must be optimized with respect to the power output: the width of the magnetW_{mag}, the width of the back iron sheet W_{sheet} and the outer diameter of the coil D_{coil} . The value for L_{mag} and L_{sheet} is equal to H_{sheet} . The inner diameter of the coil is 2 mm.

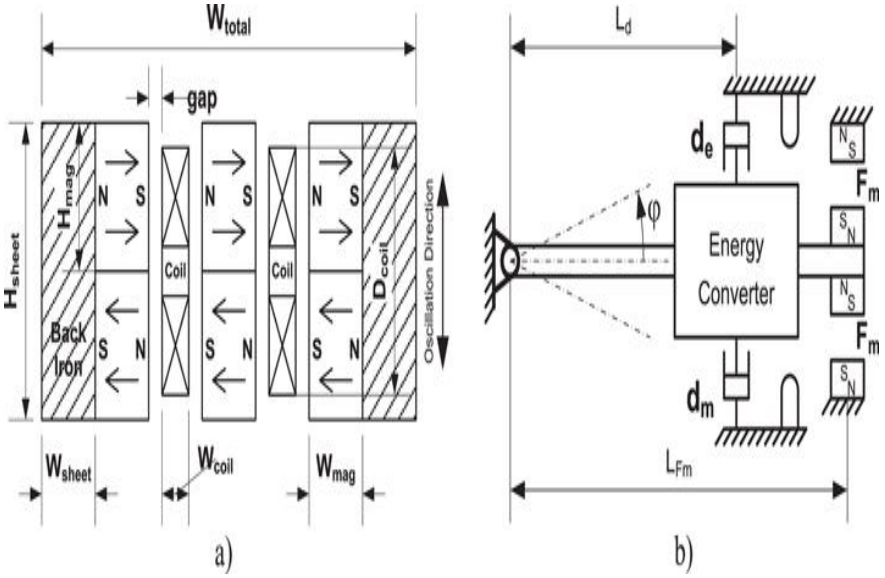

Figure 2.11 Shock-Excited energy Harvester.

In the figure 2.11 (a) is the schematic diagram (cross-section) of the active energy conversion structure showing the magnetic circuit and coils, and (b) is the simplified model of the energy harvester including the nonlinear force *F*m of the magnetic spring, mechanical stoppers and electrical and mechanical damping.

The energy conversion structure of the shock-excited energy harvester is suspended using two pairs of magnets with opposite polarity. The outer suspension magnets are fixed within the housing (base and lid). The size of the magnets can be varied for adjusting the magnetic suspension force with respect to the excitation conditions. Larger or smaller magnets will change the stiffness in the system and thus the Eigen-frequency can be varied.

For optimization of the variable design parameters a system model based on differential equations was developed and implemented in MATLAB/Simulink. A schematic diagram of the system model is shown in figure (2.11(b)). The rotational motion of the cantilever arm is described by the following differential equation:

$$J\ddot{\varphi} = \sum M_i = \sum M_g + \sum M_{ex} + M_{d,e} + M_{d,m} + M_{Fm}. \quad (2.5)$$

Where $J\ddot{\varphi}$ is equal to the sum of all torsional moments in the system. The moments induced by weight are summarized as following:

$$\sum M_g = g \sum M_i \eta = g.m_{tot}.L_{eff}.\cos\varphi. \qquad (2.6)$$

Where g is the gravity of earth, m_{tot} is the total mass in the system and L_{eff} is the effective length with respect to the center of gravity of the total mass. The external excitation also generates torsional moments as described in equation (2.7):

$$\sum M_{ex} = A \sum M_i \eta = A.m_{tot}.L_{eff}.\cos\varphi. \qquad (2.7)$$

Where A is the excitation acceleration. Further torsional moments are induced by the electrical damping force $F_{d,e}$ and the mechanical damping force $F_{d,m}$. The associated moment arm is the distance L_d. The general moment is given by:

$$M_{d,j} = F_{d,j}.L_d. \qquad (2.8)$$

The index j accounts for either electrical or mechanical damping forces. The electrical damping force $F_{d,e}$, which originates from the Lorentz force, results from the coupling factor C_F and the current i in the coil:

$$F_{d,e} = C_F(\varphi) \cdot i(\varphi, \dot{\varphi}) = d_e(\varphi) \cdot \dot{\varphi}. \qquad (2.9)$$

From equation (2.9) Follows that the electrical damping force $F_{d,e}$ can be represented by a velocity proportional damping element with the electrical damping coefficient:

$$d_e = C_F(\varphi) \frac{U_{ind}}{R_{in}+R_L} \cdot \frac{1}{\dot{\varphi}} = \frac{C_F(\varphi)^2}{R_{in}+R_L}. \qquad (2.10)$$

In the same way, the mechanical damping force $F_{d,m}$ is proportional to the angular velocity with the mechanical damping coefficient d_m:

$$F_{d,m} = d_m \cdot \dot{\varphi}. \qquad (2.11)$$

The mechanical damping coefficient was determined experimentally. The magnetic force F_m between the repulsive magnets changes with the variable in a nonlinear manner and introduces stiffness into the system. The magnetic force hereby generates a torsional moment as following:

$$M_{Fm} = F_m(\varphi) \cdot L_{Fm} \ . \qquad (2.12)$$

The magnetic force as a function of displacement angle was numerically calculated using the FE-method. The set of equations described above represents the model of the shock-excited energy harvester and was solved numerically.

The implementation of the shock-excited energy harvester is shown in figure 2.12 (the lid is removed). The rim of the housing is reinforced using steel bolts in order to increase the robustness of the device figure (2.12 (a)). The outer suspension magnets are accommodated in the base and the lid. Between the anchor and the active structure is enough space for a power management circuit. Figure(2.12(b)) shows a side view of the energy harvester structure. The device was integrated into the sole of a shoe for characterization and testing.

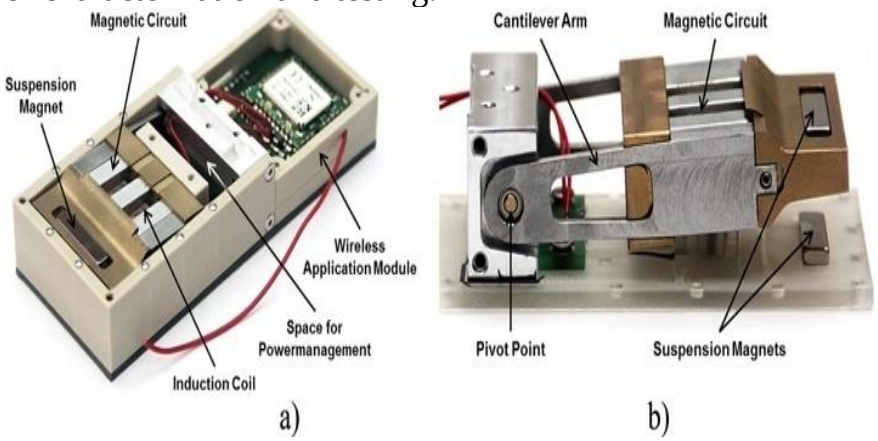

Figure 2.12 Implementation of the shock-excited energy harvester: (a) complete device (lid removed) including power management and wireless application module (b) side view showing the oscillating cantilever arm including magnetic circuit and suspension magnets.

2.6.2 Characterization

The shock-excited energy harvester was tested under realistic conditions on a treadmill. An example of the instantaneous voltage output during one step is depicted in figure (2.13(a)). The overlaid acceleration signal shows an initial acceleration peak of about 18 g, which is caused by the heel-strike. The motion speed was 6 km h−1. The highest voltage peak is about 5.8 V and corresponds to a power output peak of 46 mW (reached at the third peak in figure (2.13(b)). During one step the active structure of the shock-excited energy harvester oscillates with about 16 periods of oscillations until the voltage amplitude drops below 1 V. The decay of the voltage response seems to be a more or less linear characteristic. A second displacement event of the active structure occurs 0.65 s after the first impact. At this moment the foot is lifted from the ground. However, the power output from this event is rather small.

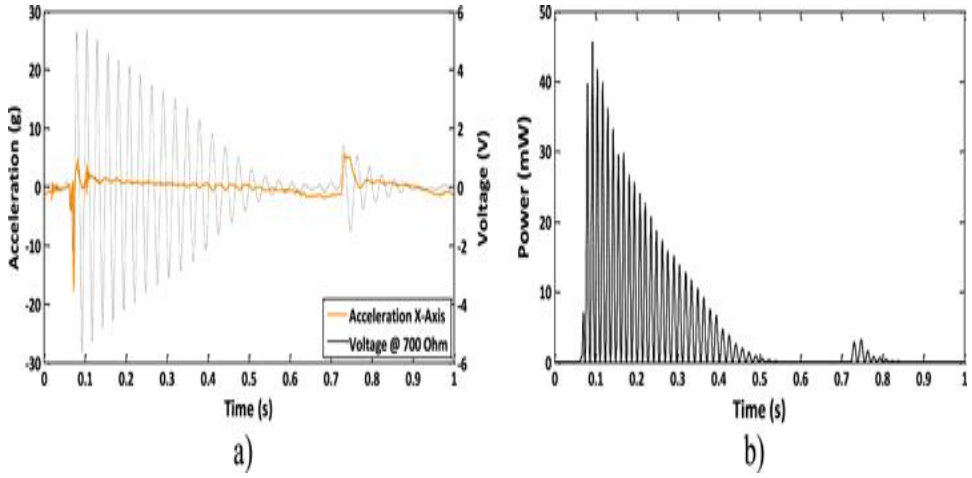

Figure 2.13 (a) Voltage output with overlaid acceleration signal from a single excitation pulse at a motion speed of 6 km h−1; (b) corresponding power output.

Figure2.14 shows the power output for two different test persons as a function of walking speed. In general the power output at a specific motion speed depends on the test subject. At a motion speed of 4 km h−1 (slow walking) the power output is 1.25 mW for test person DH whereas just 1 mW is generated for test person XY. At motion speeds of 6 km h−1 (fast walking) and 8 km h−1 (slow jogging) a more significant difference in output power can be observed between the two test persons. Possible reasons are the differences in the walking style and in the physiognomy (e.g. weight of person, length of leg, etc) of the test persons. The maximum power output of ca. 3.5 mW appears for runner XY at a motion speed of 6 km h−1 figure (2.14(b)). At a motion speed of 10 km h−1the output power is just below 3 mW and is almost equal for both test persons. At this particular motion speed, the average of the acceleration peaks from heel-strike reaches up to 34 g. In addition to the treadmill runs, the power output was also measured for 'ground walking'.

The maximum achieved power output was 4.13 mW at a motion speed of approximately 5 km h−1.

The simulation results obtained by the numerical model are also shown in figure 2.14. The power estimation is reasonably close to the experimental results. However, the drop in power output when the transition from the abrupt movements of fast walking to the smooth movements of slow jogging occurs is not apparent in the simulation data.

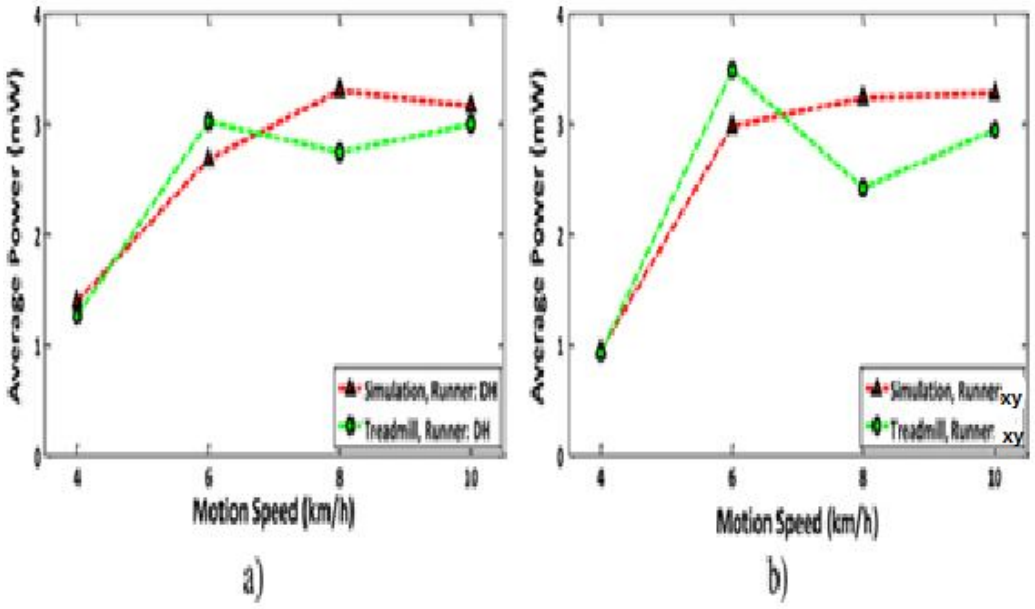

Figure2.14. Average power output (simulation and measurement) at different motion speeds: (a) runner DH; (b) runner XY.

2.7 Harvester Comparison and Conclusion

Two inductive harvesters based on different transduction principles were presented in this work. The first harvester exploits the swing motion of the foot to accelerate a magnet stack through a set of coils, while the second device employs frequency up-conversion to excite a spring-loaded magnetic circuit into resonance upon heel strike. Although based on different physical principles, both devices show similarities in the patterns of the power outputs. There is a drop in power output for both devices when the transition from the abrupt movements of fast walking to the smooth movements of slow jogging occurs. Both devices show a dependence of the test person. The more pronounced effect in the case of the swing-type harvester can be observed in the energy generated per step shown in figure 15. The fact that the shock-type harvester shows an equal generated energy for both runners towards higher motion speeds figure(2.15(b)) may be attributed to the limited inner amplitude of the device, as the magnet swing reaches this limit at relatively low motion speeds and therefore limits the generated energy.

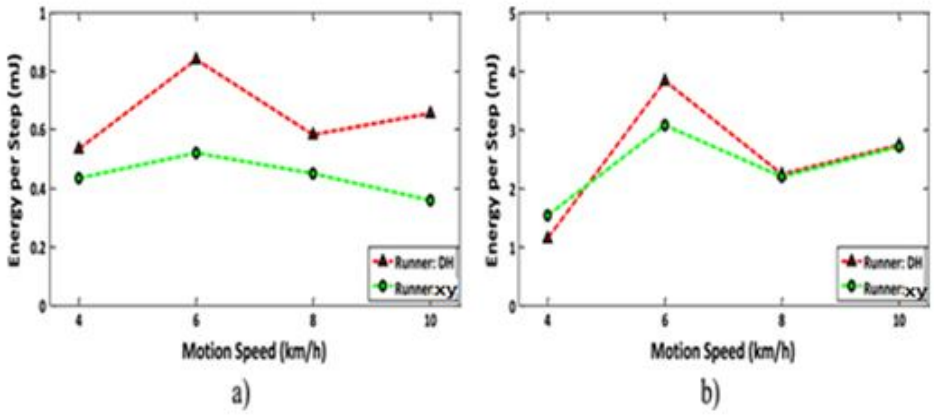

Figure 2.15 Average energy harvested 8per step for both runners: (a) swing type harvester; (b) shock-excited harvester.

Difficulties arise for the shock-type harvester when the angle between the shoe and ground upon heel strike is considered. As the heel strike generally occurs at an angle, the energy is only partially coupled into the harvester built horizontally into the shoe sole. The swing type harvester is mainly limited by the freedom of motion of the magnet stack and hence the device length, which greatly affects the power output. The height constraint also limits the coupling as the coils surrounding the magnet stack are limited to flat structures, which in turn reduces the electrical damping of the magnet motion and thus the converted energy.

The highest average power output of 4.13 mW was measured on ground at a motion speed of 5 km h−1 for the shock-type harvester, while the highest measured average power of the swing-type harvester was 0.84 mW at a motion speed of 6 km h−1on a treadmill. Considering the device volume (including housing) of 48 Cm^3 for the shock-type harvester and 21 Cm^3 for the swing-type harvester, this translates into a power density of 86 μ WCm^{-3} and 40 μ WCm^{-3} respectively.

One can see from the presented data that a reasonable power output can already be achieved at low motion speeds, with the data indicating that fast walking (6 km h−1) appears to offer the most energetic gait pattern within the considered range of speeds. However, a larger group of test subjects would be required to more precisely attribute the observed effects to the body geometries or gait styles.

In the case of the swing-type harvester, an improved model is in development which can handle a flexible and independent number of coils and magnets. First calculations have confirmed a significant increase in power output. A new optimization will be performed with the improved model and it is expected that a new prototype could close the power output gap to the shock-type harvester.

Chapter Three

PIEZOELECTRIC TRANSDUCER (MODEL DESIGN)

Chapter Three

Piezoelectric Transducer (Model Design)

3.1 preface

this chapter is going to show the study and calculate the walking force In the module using piezoelectric transducer, also study the kinetic features, we evaluated major motions performed during walking and identified the amount of work the body expends and the portion of recoverable energy. During walking, there are phases of the motion at the joints where muscles act as brakes and energy is lost to the surroundings. During those phases of motion, the required braking force or torque can be replaced by an electrical generator, allowing energy to be harvested at the cost of only minimal additional effort. The amount of energy that can be harvested was estimated experimentally and from literature data. Walking is the most common activity in human life. When a person walks, he loses energy to the road surface in the form of impact, vibration, sound etc, due to the transfer of his weight on to the road surface, through foot falls on the ground during every step. This energy can be tapped and converted in the usable form such as in electrical form. This device, if embedded in the footpath, can convert foot impact energy into electrical form. Recommendations for future directions are made on the basis of our results in combination with a review of state-of-the-art biomechanical energy harvesting devices and energy conversion methods. a Couple of suggestions has been made to increase the efficiency and accuracy of the steps walking and in the end the piezoelectric element design and in the end the power generated from the piezoelectric transducer and usage of the power in mobile electronics device are shown and modulated through several computer programs which will be disused briefly in the next chapter.

3.2 Components of the Project and Circuit Diagram

3.2.1 Piezoelectric Element

In general all piezoelectric elements are the same; it refers to the discrete component that produces current when actuated. They are also known as ceramic transducers and are usually found in outdated pairs of earpiece which is the ability of certain materials to generate an AC (alternating current) voltage when subjected to mechanical stress or vibration, or to vibrate when subjected to an AC voltage, or both. The most common

piezoelectric material is quartz. Certain ceramics, Rochelle salts, and various other solids also exhibit this effect.

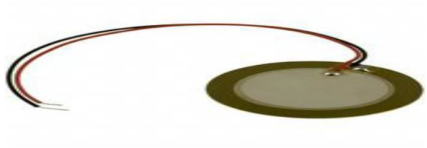

Figure 3.1 Piezoelectric transducer making power from pressing

3.2.2 Rectifier

Usually is composed of four rectifier diodes that filter AC currents and turn them into DC currents. The rectifier circuit is shown in the figure (3.2). The circuit has four diodes connected to form a bridge. The ac input voltage is applied to the diagonally opposite ends of the bridge. The load resistance is connected between the other two ends of the bridge. In this project, a bridge rectifier is used because of its merits like good stability and full wave rectification. The rectifier is a circuit, which converts an ac voltage to dc voltage using both half cycles of the input ac voltage.

3.2.3 Capacitor

Capacitor usage to smooth the output power that induced through the rectifier and starting charging the capacitor then to save time. The amount of the capacitor which used in the experiments is 22μF as showing in the calculations part is the suitable amount to charge a battery.

3.2.4 Voltammeter

Usually is used to measure voltage that induced from the walking through the piezoelectric sensor power and making the calculations of the power outage.

3.2.5 Electrical Switch

To control the power induced through the four ways rectifier either to go through LED cell to show the power density or to save the power in the capacitor and use it to charge any electronic devices.

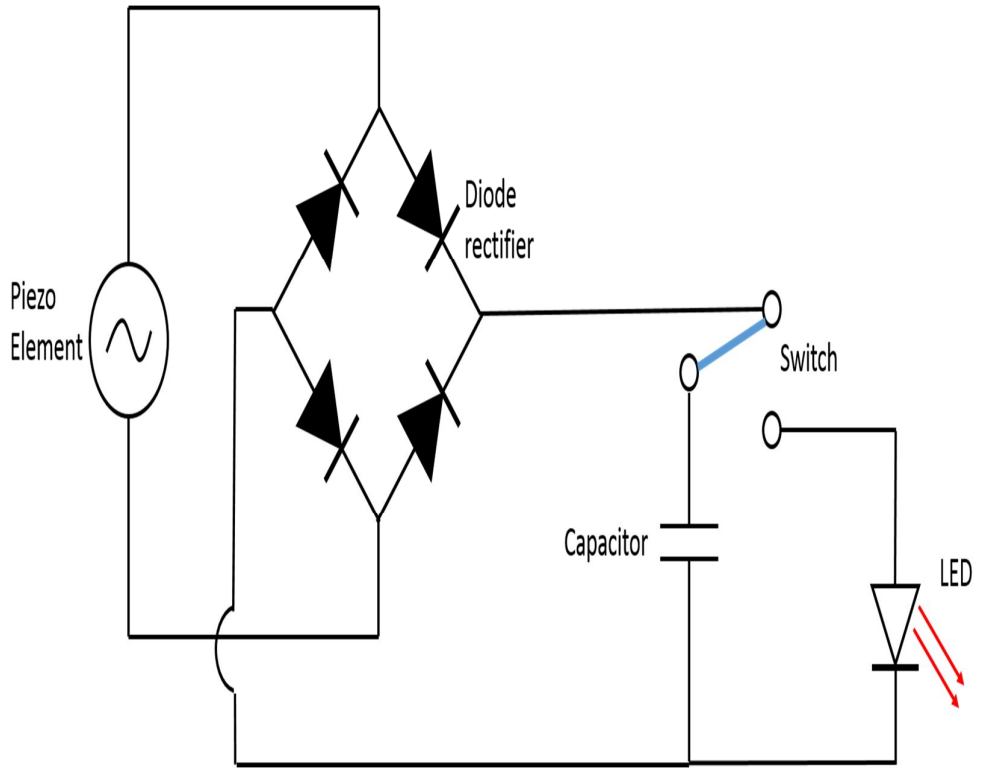

Fig 3.2 Power from walking using a piezoelectric energy circuit diagram

After building the circuit which consists of the above element and then the circuit will be connecting as the following:
The positive terminal of the piezoelectric element will be connecting with the 4 ways rectifier which will be connecting to the electrical capacitor then the researcher will put the piezoelectric element inside the boot under my Hansel so when step down on it force is applied and then released small voltage will appear throughout the rectifier and start charging up the capacitor. The key is to control whether you want to display the density of light that generates from the piezoelectric or not!

3.3 The Calculations

Then after a 57 steps I get 21.7 volts now here the calculations:
To calculate energy from the capacitor:

$$E = \frac{1}{2} . v^2 . c$$

Where:

V: The Voltage
C: Capacitance
E: Energy

$$E = \frac{1}{2} . 21.9^2 . 22\mu F$$

=0.00528 j
= 5.28mj
E/step= 5.28mj/ 57step = 92.5μj
92.5μj per step is very small amount of energy.
The cell phone battery holds a 4.7 w h which is the equivalent of 16.92kj
4.7 w h = 16.92 k j
= 16,920 j
= 0.0000925 j
After making this calculation we conclude the number steps that charge a cell phone battery that it would take: 182 million steps.
Then we studied another application which needs fewer steps to make it easier because it would be difficult for one person to get that much in small duration while of course if we made this project in a disco hall it will takes less than an hour. The application that needs a few steps is a battery lighter and then the calculation will be as following:

$$E = \frac{1}{2} . v^2 . c$$

$$E = \frac{1}{2} . 3^2 . 22\mu F$$

=0.000099 j
= 0.0001 =0.1 mj
E/step= 0.1mj/ 57step = 1.75μj
Then from all that examples we conclude that the output will get from the piezoelectric transducer (the harvester) depending on the application that we want to apply so that I made a simulation for the mechatronics model so that we will have the actual results.

3.4 Summary

Our theoretical calculations align well with current device performance data. Our results suggest that the most energy can be harvested from the lower limb joints, but to do so efficiently, an innovative and light-weight mechanical design is needed. We also compared the option of carrying batteries to the metabolic cost of harvesting the energy, and examined the advantages of methods for conversion of mechanical energy into electrical energy and then use it to charge a cell phone battery which becomes now the principle of charging whatever electronic device that need regularly or partially to be charged on a daily basis and so on by amplifying the electrical power using a specific type of amplification depending on the device, or even use it as it is.

Chapter Four

SYSTEM MODELING AND SIMULATION

Chapter Four
System Modeling and Simulation

4.1 Preface

Structure of the powering a mobile electronics by using a piezoelectric transducer was designed and analyzed using new analysis program (the program that the researcher suggest it is mikro c simulation of electrical circuits or else can pit one of the new techniques of the Nanotechnology harvesting energy and even by using Matlab Simulink then the result of the simulation was showing in the following paragraphs.

4.2 Simulation of The Harvester Using Proteus8

By using mikro C proteus for PIC and orduino simulation the electrical circuit will be as the following considering all that and in the same time the idea explained much better in appendix part….

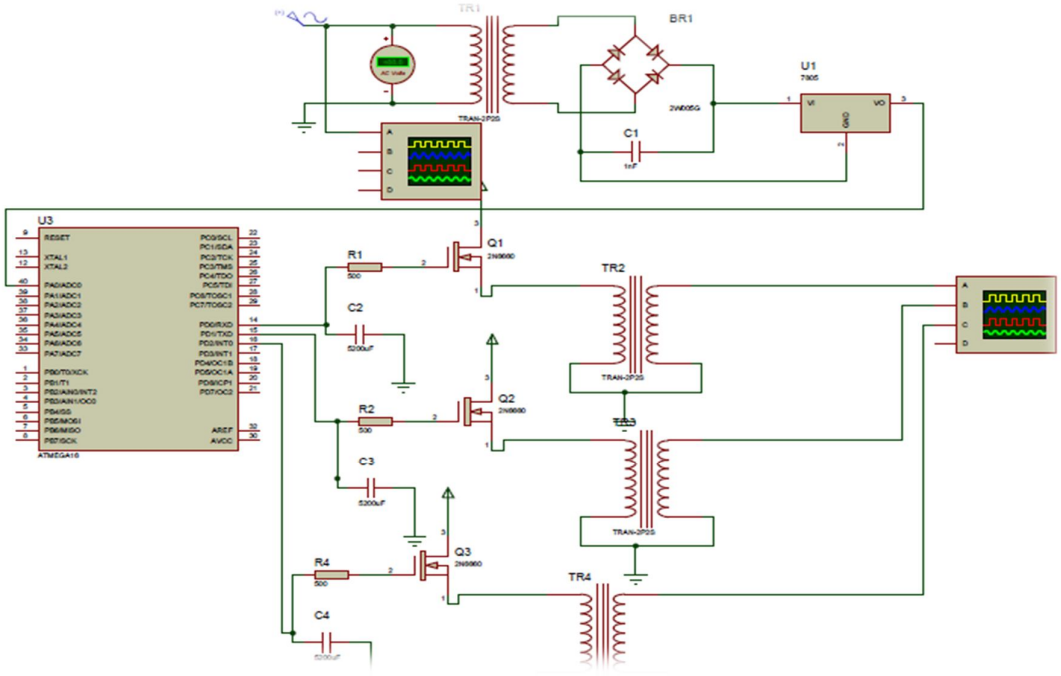

Fig 4.1 Simulation and Modeling of the Harvester Making Power from Walking.

The idea was to attach an Arduino development board to establish a simple oscilloscope setup so that to plugged to the computer; the built-in TTL was used to establish serial communication between the Arduino

and PC. A sketch was uploaded, using the Arduino IDE, to monitor the Analog pin where the insole generator was connected. A separate program, called "processing 2.0", was used to monitor the ripple given off by the converted AC to DC output of the generator.

The output from the transformer is fed to the rectifier. It converts A.C. into pulsating D.C. The rectifier may be a half wave or a full wave rectifier. In this pro project, a bridge rectifier is used because of its merits like good stability and full wave rectification. The Bridge rectifier is a circuit, which converts an ac voltage to dc voltage using both half cycles of the input ac voltage. The Bridge rectifier circuit is shown in the figure. The circuit has four diodes connected to form a bridge. The ac input voltage is applied to the diagonally opposite ends of the bridge. The load resistance is connected between the other two ends of the bridge. For the positive half cycle of the input ac voltage, diodes D1 and D3 conduct, whereas diodes D2 and D4 remain in the OFF state. The conducting diodes will be in series with the load resistance RL and hence the load current flows through RL.

For the negative half cycle of the input ac voltage, diodes D2 and conduct whereas, D1 and D3 remain OFF. The conducting diodes D2 and D4 will be in series with the load resistance RL and hence the current through RL in the same direction as in the previous half cycle. Thus a bi-directional wave is converted into a unidirectional wave.

4.3 Simulation Summary

current results showed that the product has potential to charge lithium batteries. Though there are rooms for improvements, it showed The positive signs for it to be further developed. Based from the results, the insole generator has enough power to supply voltage for low powered circuits such as MCUs (Micro Controller Units - ex. ATtiny) and TTL Bluetooth transmitters. I can now say that the product is ready for production and is highly usable for smart clothing/ shoes. Charging USB devices won't suffice just yet, the charging time just isn't ideal.

1. The project “POWER GENERATION USING FOOT STEP” is successfully tested and implemented which is the best economical, affordable energy solution to common people.

2. This can be used for many applications in rural areas where power availability is less or totally absence As India is a developing country where energy management is a big challenge for huge population. By

using this project we can drive both A.C. as well as D.C loads according to the force we applied on the piezo electric sensor.

Basically a good piezoelectric element (the harvester) has to be designed accordingly. In turn this requires a certain minimal device size as the power output of the harvester system is directly related to the size of the electromechanical transducer. In the case of inductive harvesters this could for example translate into large magnets and in piezoelectric devices into a large number of active layers.

As a matter of consideration for device design we obtained results showing the amount of positive and negative muscle work in each motion, and motion where energy is lost to the surroundings (e.g., heel strike). The importance of these results is that they will affect the design of energy-harvesting devices.

Chapter Five

CONCLUSION AND RECOMMENDATION

Chapter Five

Conclusion and Recommendation

5.1 Conclusion

The idea of power harvesting has become increasingly popular over the past few decades. With the advances in wireless technology and low power electronics, portable electronics and remote sensors are now part of our everyday lives. The key to replacing the finite power supplies used for these applications is the ability to capture the ambient energy surrounding the electronics. Piezoelectric materials form a convenient method of capturing the vibration energy that is typically lost and converting it into usable electrical energy. This material has been used in
The power harvesting field for some time; however, the energy generated by these materials is far too small for directly powering most electronic systems. This problem has been found by most all researchers that have investigated this field, thus showing the need for methods to accumulate the generated energy until a sufficient amount is present. Typically the storage medium used has been the capacitor, but the capacitor is not a good source to reserve the energy because there are losses accursed their surfaces.
Perhaps the most magical method of energy harvesting is drawing on ambient electromagnetic emissions. This isn't a new idea: Crystal radios were pretty popular once upon a time, and RFID tags and photovoltaic cells are pretty popular today. The concept can be taken further, however. It is possible to pull energy from the various radio frequencies that wash over us all the time. The Spanish textile research association Aitex, in collaboration with other researchers, has created cloth that contains tiny antennas woven directly into the fabric. This technology could be developed so that our clothing could capture enough energy to power biometric sensors and other wearable devices. Thus it is only an excellent example of how the whole can be greater than the sum of its parts. There was an energy and enthusiasm among the participants that's been missing at many technology events in recent years. The excitement generated by the multiple markets, all experiencing rapid growth, was reminiscent of the heady early days of the personal computer, when anything was possible and amazing products were within reach. Energy harvesting is going to play an important role in changing the way we interact with everyday items, our data, one another, and even our own bodies.

The method of getting the energy from walking which is the most common activity in human life. When a person walks, he loses energy to

the road surface in the form of impact, vibration, sound etc, due to the transfer of his weight on to the road surface, through a piezoelectric transducer falls on the ground during every step. In the whale thesis we studied the possibility and how we can use the electrical energy induced from walking to charge electronic devices depending on its function.

5.2 Recommendation

1. The design can be improved by implementing sensory so that error can be compensated.
2. One can also study the piezoelectric actuated techniques and compare the results with results obtained in this work.
3. Biomechanical energy harvesting constitutes clean, portable energy alternative to conventional batteries for electronic mobile devices. High-power medical devices, such as prostheses with electrical motors and controllers and exoskeletons, could certainly also benefit from the development of this technology.
4. The foot stepper can be used while the person is walking as well as while doing any activity by butting the device under the Hansel of the shoe to charge a cell phone battery even if the device is charged then in this case the energy to be harvested whenever the human needs to charge his phone even if there is no electricity he has a harvested one in his power band that generated while walking let's say from his car to inside the building of his office and going back later

References

[1] Ramsay M J and ClarrkW W Piezoelectric energy harvesting for bio MEMS applications Proc. SPIE 4332 429–38, 2001.

[2] Starner, T.,"Human-Powered Wearable Computing," IBM Systems Journal, Vol. 35, pp.618,1996.

[3] Stephen R. Platt, Shane Farritor, and Hani Haider "On Low-Frequency Electric Power Generation with PZT Ceramics .

[4] V. Hugo Schmidt, "Piezoelectric energy conversion in windmills," in Proc. Ultrasonic Symp., pp. 897–904, 1992.

[5] Minhang Bao, analysis and design principles of MEMS devices, pp 247 -253.

[6] Starner T Low-Power Electronics Design (Boca Raton: CRC Press) ch 45, 2005.

[7] Niu P, Chapman P, Riemer R and Zhang X Evaluation of motions and actuation methods for biomechanical energy harvesting IEEE 35th Annual Power Electronics Specialists Conf. 2100–6, 2004.

[8] Kymissis J, Kendall C, Paradiso J and Gershenfeld N 1998 2nd Int. Symp. Wearable Computers 132–9.

[9] Bai P, Zhu G, Lin Z-H, Jing Q, Chen J, Zhang G, Ma J and Wang Z L Integrated multilayered triboelectric nanogenerator for harvesting biomechanical energy from human motions ACS Nano 7 3713–9f, 2013.

[10] Bramhanand A and Kim H Micro fluidic energy harvesting system for high force and large deflection accomodation PowerMEMS 2011 Proc.—Seoul (Republic of Korea,) 74–7, 2011.

[11] Paradiso J A and Starner T Energy scavenging for mobile and wireless electronics IEEE Pervasive Comput. 4 18–27, 2005.

[12] Krupenkin T and Taylor J A Reverse electrowetting as a new approach to high-power energy harvesting Nat. Commun. 2 448, 2011.

[13] Pillatsch P, Yeatman E M and Holmes A S A scalable piezoelectric impulse-excited energy harvester for human body excitation Smart Mater. Struct. 21 115018, 2012.

[14] Moro L and Benasciutti D Harvested power and sensitivity analysis of vibrating shoe-mounted piezoelectric cantilevers Smart Mater. Struct. 19 115011, 2010.

[15] Ylli K, Hoffmann D, Folkmer B and Manoli Y Design, fabrication and characterization of an inductive human motion energy harvester for application in shoes J. Phys.: Conf. Ser. 476 12012, 2013.

[16] Carroll D and Duffy M Modelling, design, and testing of an electromagnetic power generator optimized for integration into shoes Proc. Institution of Mechanical Engineers: I. Journal of Systems and Control Engineering 256–70 vol 226, 2012.

[17] Spreemann D and Manoli Y Electromagnetic Vibration Energy Harvesting Devices: Architectures, Design, Modeling and Optimization (Dordrecht, New York: Springer,2012 .

APPENDEX

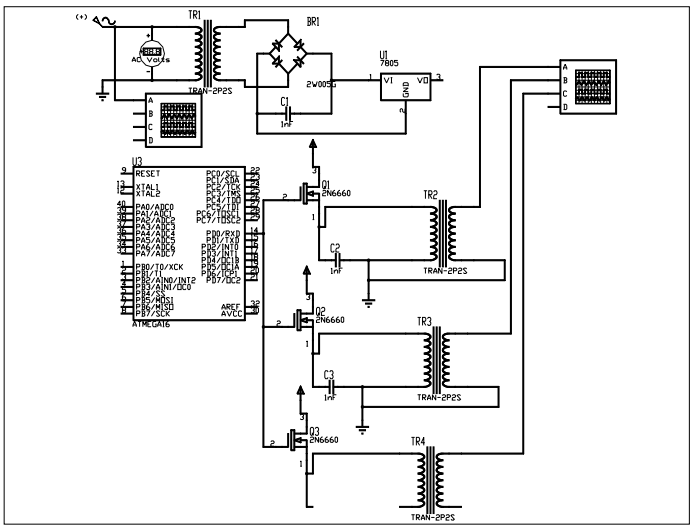

Which contains of the simulation of the foot stepper the electrical circuit is the first part of the appendix that After building the circuit which consists of the above element and then the circuit will be connecting as the following: The positive terminal of the piezoelectric element will be connecting with the 4 ways rectifier which will be connecting to the electrical capacitor then I will put the piezoelectric element inside the boot under my Hansel so when I step down on it force is applied and then released small voltage will appear throughout the rectifier and start charging up the capacitor. The key is to control whether you want to display the density of light that generates from the piezoelectric or not!

And the connection of the second part is the electronic circuit to show The output from the transformer is fed to the rectifier. It converts A.C. into pulsating D.C. The rectifier may be a half wave or a full wave rectifier. In this pro project, a bridge rectifier is used because of its merits like good stability and full wave rectification. The Bridge rectifier is a circuit, which converts an ac voltage to dc voltage using both half cycles of the input ac voltage. The Bridge rectifier circuit is shown in the figure. The circuit has four diodes connected to form a bridge. The ac input voltage is applied to the diagonally opposite ends of the bridge. The load

resistance is connected between the other two ends of the bridge.

For the positive half cycle of the input ac voltage, diodes D1 and D3 conduct, whereas diodes D2 and D4 remain in the OFF state. The conducting diodes will be in series with the load resistance RL and hence the load current flows through RL.

For the negative half cycle of the input ac voltage, diodes D2 and D4 conduct whereas, D1 and D3 remain OFF. The conducting diodes D2 and D4 will be in series with the load resistance RL and hence the current flows through RL in the same direction as in the previous half cycle. Thus a bi-directional wave is converted into a unidirectional wave.